ANALYSIS OF THE INFLUENCE OF VISCOELASTICITY IN CURL DEVELOPMENT IN SLS

NM Jamal & KW Dalgarno

School of Mechanical Engineering, University of Leeds, Leeds, LS2 9JT, UK.

Abstract

Curl in selectively laser sintered parts arises mainly from thermal distortion of parts within the build volume during processing. This results in nominally flat surfaces which lie horizontally in the part bed becoming warped. This paper reports on the use of finite element techniques to model curl development in polymer materials, and in particular on the influence of viscoelasticity on how curl develops. The development of time-dependent material models is reported, and the results of the implementation of these models presented, together with a comparison of the results with experimental data.

Introduction

In common with most rapid prototyping processes, SLS does not produce parts as accurately as more conventional manufacturing processes, with accuracies of ± 0.2 mm commonly quoted [1]. Inaccuracy in SLS can arise from (i) data exchange, (ii) the inherent mis-match between a 3D object and a collection of 2D layers, (iii) the resolution of the laser and laser positioning system, and (iv) shrinkage and warping as a result of the distributions of thermal energy and melting/solidification mechanisms [2]. Choi and Samavedam [2] have noted that it is the last of these sources of inaccuracy which are currently least well understood, and present methods by which sources (i) to (iii) can be minimised.

One result of shrinkage and warping in SLS is the phenomena known as curl, which results in nominally flat surfaces which lie horizontally in the part bed becoming warped. Figure 1 illustrates this schematically. Previous work on the selective laser sintering of polycarbonate [3] has identified two major regions of curl within a part. The first of these appears over approximately the 2.5 mm of part closest to the edge of the part and on parts of with the geometry shown in Figure 1 has a radius (R_I in Figure 1) of around 20 mm. The second extends from the end of R_I approximately 10 mm further towards the centre of the part and has a radius (R_{II} in Figure 1) of around 60 mm. R_I curl has been seen to exist from the sintering of the first layer in part build, while R_{II} curl develops as layers are added to the part. R_I curl is considered to arise from densification and shrinkage effects during processing of the first layer, whereas R_{II} curl is believed to arise from thermally induced stresses which develop as subsequent layers cool onto layers which have already been processed [4].

Previous work [5] attempted to model R_{II} curl development in the SLS of polycarbonate using finite element methods, and did provide some insight into the mechanism of curl development. However, within these models assumptions were made regarding the material properties, and, in particular, no account was taken of the effects of viscoelasticity. The aim of the work described in this paper was to develop improved finite element models in order to provide greater understanding of curl development.
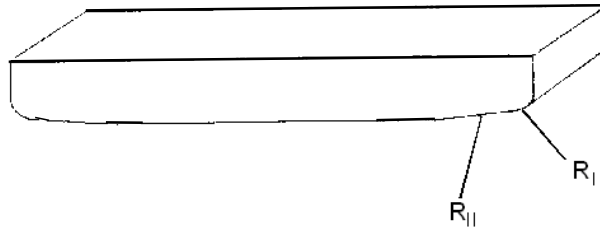
Figure 1 - Effect of Curl on Component Geometry of a 90 x 25 x 7 mm Part

Approach to Analysis

Analysis of curl development in SLS requires that a coupled thermal-stress analysis be used. Such analyses can be either sequentially coupled, where the results of a heat transfer analysis is used to provide temperature data to a stress analysis, or fully coupled, where the heat transfer and stress analyses are solved simultaneously. A sequentially coupled analysis may be performed where it can be assumed that the thermal analysis would not be affected by the results of the stress analysis, and this assumption has been made in the work reported here.

The models were based on the manufacture of a simple test part on a DTM Sinterstation 2000, in which individual layers were 90 x 25 mm in area, and ten layers, of nominal thickness 0.127 mm, made up the part. The laser power, laser speed, and scan spacing were 11 W, 1188.87 mm/s, and 0.25 mm respectively. The f.e. code used was ABAQUS. This code allows for elements to be activated and deactivated through the course of an analysis, which was used to simulate the addition of material, and also has a wide range of material models, which were of value in modelling viscoelasticity.

Heat Transfer Analysis Results

The heat transfer modelling is reported in full elsewhere [6]. As the main purpose of this paper is to examine the effects of viscoelasticity, emphasis will be placed on the stress analysis and only relevant results from the heat transfer analysis are presented. The heat transfer analysis considered both the part itself and the powder bed, and Figure 2 shows the temperature results from the heat transfer model for a typical layer deposition/heating/lasing/cooling sequence, and for final cooldown. In Figure 2 (a) the points in time at which the elements making up a particular layer were activated are illustrated, as is the instant at which sintering was modelled.

Stress Model - Geometry

Figure 3 shows the f.e. mesh used in the stress analysis. As for the thermal analysis a 2D representation has been used, with advantage taken of symmetry to half the size of the model. Within the stress analysis the powder bed was not considered to have any significant influence on the distortion of the manufactured part, and so the stress analysis considered only the manufactured part itself. In modelling the powder bed it has been assumed that the most significant effect the powder bed would have would be in restricting the contraction and expansion of the layers in the x direction, with the powder expected to have little influence on the behaviour of the part in the z direction. This led to the use of a rigid surface to represent the powder bed, as this allows frictional behaviour between the part and powder bed to be specified,

350

whilst the rigid assumption removes the need for any interaction between part and powder bed in the z direction. It can also be seen in Figure 3 that the four rows of elements are used to make up layer 1, with one row of elements for each of the subsequent layers: this reflects the effect of bonus-z, and the layer thicknesses used are based on experimental measurement of the thickness of parts with the same section, but comprising 1 to10 layers [6]. The nodes forming the elements shown in Figure 3 were augmented by a set of "dummy" nodes between elements which allowed elements, when activated, to be activated in a stress free state, following standard modelling practice [7]. The elements used were four noded plane strain (CPE4I), with rigid surface (IRS21) elements used to represent the interface between the surface and the part.
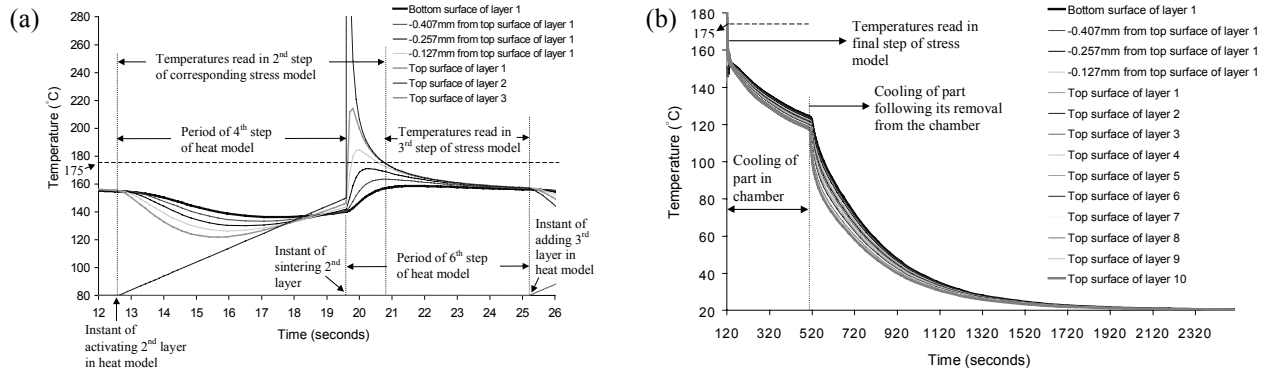
Figure 2 - (a) Thermal Model Results Over Second Layer Addition, Sintering and Cooling, and (b) Thermal Model Results from Cooldown

Stress Model - Material Properties

The stress model required that the density, coefficient of friction between part and powder bed, the coefficient of thermal expansion, the modulus and Poisson's ratio, and the time dependent mechanical properties be defined. The density of the part was measured to be 497 kg/m^3, and the coefficient of friction between the bottom surface of the part and the powder bed was defined as 0.38, based on experimental measurement at room temperature [6]. The development of an appropriate value for the coefficient of thermal expansion proved difficult. A standard value for polycarbonate would be 6.5 x 10^{-5} /°C, however this value had previously been found [5] to grossly overestimate curl, with a value of 2 x 10^{-6} /°C more representative of the behaviour observed in SLS, and this value was also adopted in the work reported here. This value was applied to all elements except the lower two rows shown in Figure 3. The thermal model indicated that the average nodal temperatures in these elements did not exceed the glass transition temperature (175°C). This, allied to observation by Ho et. al. [8] that this area of layer 1, which in effect represents part of the bonus-z, was only lightly fused, led to the assumption that the expansion coefficient would be very low in this region, and so the expansion coefficient for these two rows of elements was set to zero. To develop values of the instantaneous modulus tensile tests at a range of temperatures were carried out, and the results of these can be seen in Table 1. The f.e. code used linear interpolation to develop modulus values throughout the temperature range. Modulus values above a temperature of 150°C could not be obtained, and it was assumed that above this temperature the modulus value measured at 150°C applied. A Poisson's ratio of 0.385 was used, based on room temperature measurements reported by Bushko and Stokes [9]. The time dependent response of the polymer was defined in the stress model

through a viscoelastic material model which forms part of the ABAQUS code. This initially simulates the time dependent response at a reference temperature based on stress relaxation data provided at that temperature, and then employs the WLF approximation to predict the time dependent response at all other required temperatures [10].
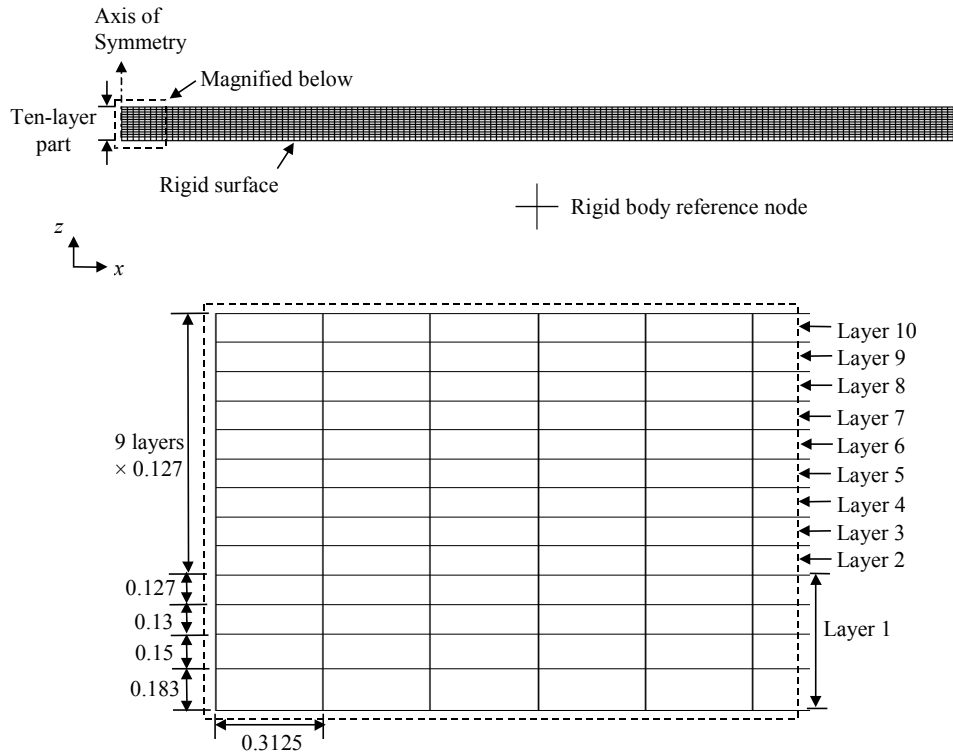
Figure 3 - Stress Analysis Mesh. Dimensions in mm.

Temperature (°C)	20	120	135	140	145	147	150
Modulus (MPa)	329.3	221.4	204	106	61	38.4	11.8

Table 1 - Measured Instantaneous Modulus Values

The reference temperature behaviour was modelled using the Prony series, which is based on n spring/dashpot Maxwell elements in parallel [11] and can be expressed as,

$$\frac{E(t)}{E_o} = 1 - \sum_{i=1}^{n} \frac{E_i}{E_o}\left(1 - \exp(-t/\tau_{mi})\right)$$

where $E(t)$ is the time dependent modulus, E_0 is the instantaneous modulus, E_i is the elasticity of the spring in the ith Maxwell element, and τ_{mi} is the relaxation time constant of that element, and t is time. The implementation of the material model in ABAQUS requires an instantaneous modulus value together with values of $E(t)$. The reference temperature employed in the analysis was 145°C, and so the instantaneous modulus at that temperature from Table 1 was used. Figure 4 (a) shows the results of a stress relaxation test – a table of values from that figure were defined in the model, and from this information the ABAQUS programme calculated the n, E_i, and τ_{mi} values which were used in the analysis.

The WLF approximation is based on the observation that E(t) curves for a particular polymer developed at different temperatures and plotted on a log time scale are similar in shape but horizontally shifted along the log time scale. This is illustrated in Figure 4 (b) for three temperatures: T_s, T_1, and T_2. This means that if the modulus-log time curve is known at a reference temperature, for example T_s, the curves at other temperatures can be estimated by applying a shift of $\log(a_T)$ on the log time scale [12]. The WLF approximation is commonly expressed as,

$$\log(a_T) = \frac{-C_1(T - T_s)}{C_2 + (T - T_s)}$$

where C_1 and C_2 are constants which must be derived for a particular reference temperature, and T is the temperature at which the modulus-log time curve is required. The WLF approximation is generally held to be accurate over the range $T_s \pm 50°C$ [11]. The reference temperature used in this study was 145°C, and from stress relaxation tests values for C_1 and C_2 of 16.47 and 115.549°C respectively were used. The development of these values in full is outwith the scope of this paper, a full treatment of their development may be found in [6].
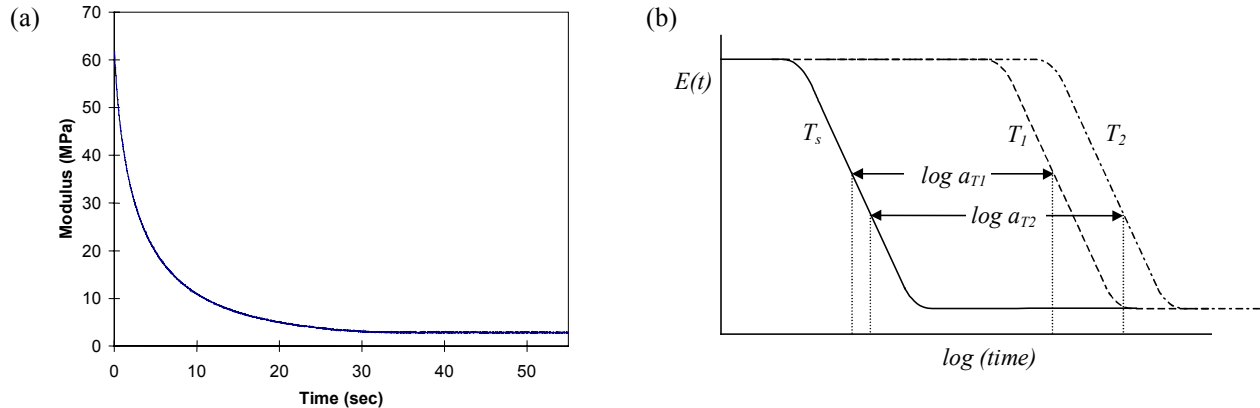
Figure 4 - (a) Stress Relaxation Test on SLS'd Polycarbonate Sample at 145ºC, and (b) Creep or Stress Relaxation Curves Obtained at Different Temperatures ($T_s < T_1 < T_2$), after [12].

Stress Analysis - Loading and Boundary Conditions

The only boundary conditions applied were to enforce symmetry on the nodes at the left hand side of the mesh, and to prevent the rigid body from movement. Two forms of loading were applied, gravity loads and thermal loads, to two types of analysis step, powder addition and sintered layer cooling.

Powder addition was modelled by adding a uniform pressure representing the weight of the added powder to then top of the active mesh, and by reading the temperature data from the heat transfer analysis through to allow the thermal strains to develop. In sintered layer cooling steps the elements forming the most recently added layer were activated, given their weight, and the uniform pressure applied in the previous step to represent their weight removed. The temperature data was also read from the heat transfer analysis, however, temperature data was only read through once the temperature had reduced below 175°C. Dynamic Mechanical Analysis testing with the polycarbonate material identified the glass transition temperature for the material to be 175°C. It was considered that the polymer would not sustain stresses at a

temperature above the glass transition temperature, and so the data from above that temperature was discarded, as shown in Figure 2 (a). In addition the values of the expansion coefficient for any part of the mesh where the temperature exceeded 175°C were set to zero.

Stress Analysis - Results

Figure 5 shows the predicted profiles of the upper and lower surfaces of the part at the end of the analysis (at room temperature). Table 2 indicates how the maximum vertical distance of the lower surface of the part changes between analysis steps within the analysis as a whole, although for brevity only the changes associated with modelling four of the layers are listed. These results show that, the addition of the colder powder causes an increase in the predicted curl, the laser sintering step causes a decrease in the predicted curl, and that as the new layer cools, the predicted curl increases again. The results also show that these effects generally reduce in scale as the number of layers increases, as the amount of material available to resist the distortion increases. Table 2 also shows that the influence of the final cooldown step on the final predicted curl is high.
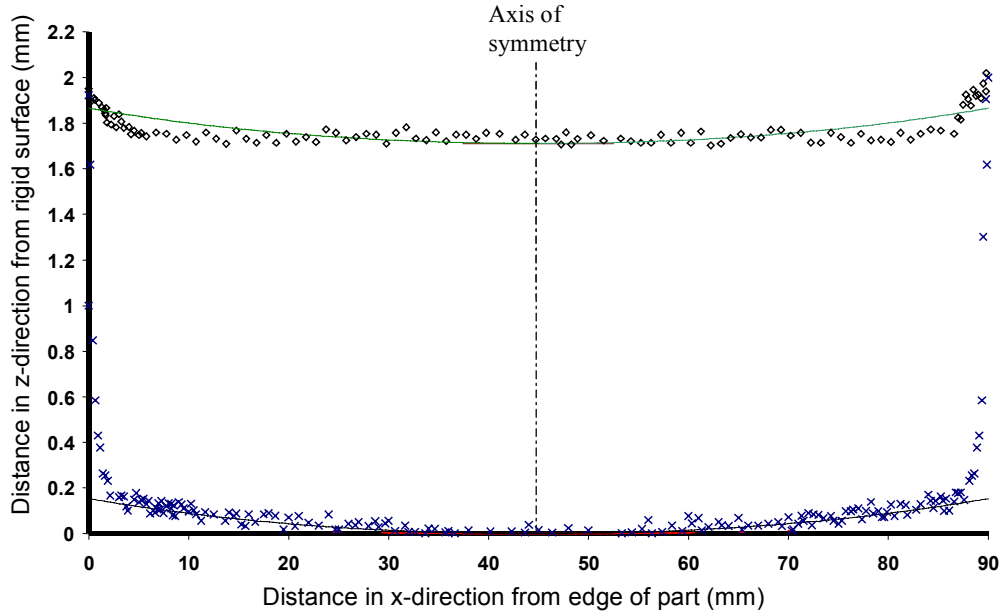
Figure 5 - ◊ Experimental Measurement of Part Lower Surface, x Experimental Measurement of Part Upper Surface. Lines Show Profiles Predicted by Analysis.

Experimental Measurement of Curl

Components with the geometry described above were manufactured using the processing conditions also described above. These were then cleaned to remove any residual powder, and the upper and lower profiles of the components measured by traversing the components under a non-contacting laser displacement meter using a flat table driven by a spring loaded micrometer. Typical results are shown in Figure 5. The results appear to exhibit scatter: in fact the apparent scatter is of the order of the powder particle size, and is considered to be a true representation of the outer surface of the components.

Discussion

Curl of the type investigated here is considered to arise in two ways - cooldown curl which generates a bulk deformation of a component as it cools from the operating temperature to room temperature, and in-build curl which only affects the lower of a part as the upper surface is continually levelled as each new layer is added. Figure 5 shows clearly that the model overestimates the cooldown curl, which, excepting the edge effect, is very small. It is believed that this is as a result of the modelling assumptions made regarding the lower two layers of elements having a zero coefficient of expansion - if these two layers of elements are given the same coefficient of expansion as the other layers then the modelled cooldown curl decreases to be of a similar order of magnitude as that observed experimentally.

Stage in Analysis	Maximum distance of bottom surface of build from the rigid surface (mm)		
	Viscoelasticity Considered		Viscoelasticity *not* considered
	Start of stage	End of stage	End of stage
Layer 1 Cooling	0	1.73×10^{-4}	2.45×10^{-3}
Layer 2 Powder Addition and Heating	1.73×10^{-4}	8.97×10^{-4}	6.55×10^{-3}
Layer 2 in melt state following sintering	8.97×10^{-4}	8.06×10^{-6}	4.95×10^{-5}
Layer 2 Cooling	8.06×10^{-6}	1.65×10^{-4}	2.21×10^{-3}
Layer 3 Powder Addition and Heating	1.65×10^{-4}	1.11×10^{-3}	1.39×10^{-2}
Layer 3 Laser Sintering	1.11×10^{-3}	2.22×10^{-5}	5.78×10^{-5}
Layer 3 Cooling	2.22×10^{-5}	1.86×10^{-4}	2.23×10^{-3}
Layer 9 Powder Addition and Heating	3.58×10^{-4}	7.4×10^{-4}	9.65×10^{-3}
Layer 9 Laser Sintering	7.4×10^{-4}	2.15×10^{-4}	7.17×10^{-4}
Layer 9 Cooling	2.15×10^{-4}	4.03×10^{-4}	3.67×10^{-3}
Layer 10 Powder Addition and Heating	4.03×10^{-4}	7.81×10^{-4}	9.23×10^{-3}
Layer 10 Laser Sintering	7.81×10^{-4}	2.82×10^{-4}	9.44×10^{-4}
Layer 10 Cooling	2.82×10^{-4}	0.1542	0.241

Table 2 - Changes in Predicted Curl Through Analysis

This means that the apparent good correlation between analysis and measurement shown in Figure 5 for the lower surface of the part is false - if the overestimated cooldown curl is removed then the analysis significantly underestimates the curl on the lower surface. This is also most likely related to the coefficient of expansion - a very low value for this was chosen on the basis of previous work with simpler material models. It is considered that the more representative material behaviour within the analysis presented here has made that assumption obselete. Further work will examine this in more detail.

The stress model with minor modifications was implemented to investigate the effect of viscoelasticity on curl. The modified model did not take into account the viscoelastic effect of the polymer, i.e. the modulus was time-independent but remained temperature dependent as specified in Table 1. Other definitions in the modified model were identical to those mentioned in the original viscoelastic stress model. Table 2 shows how the maximum distance of the bottom surface of the build, with viscoelasticity considered, compares with corresponding distances with viscoelasticity not considered. The general observation seen is that SLS operations suggested by the viscoelastic model to cause rise and reduction in curl, mentioned

above, have an identical effect if viscoelasticity is not considered. However, the results in Table 2 suggest that viscoelasticity does play a significant role in the development of curl.

Conclusion

This paper has presented an analysis of curl development in the SLS of polycarbonate which includes the definition of a full description of the viscoelastic response of the polymer. The analysis gives a qualitative insight into the development of curl, and of the effect of viscoelasticity in that, but further work is required to develop quantitative agreement with experimental observations.

References

1. Shellabear, M. Benchmark study of accuracy and surface quality in RP models. *EU BRITE/EURAM Contract No. BRPR-CT96-0155 (Process Chains for Rapid Technical Prototypes, RAPTEC) Task 4.2 Report 2,* June 1999. Downloaded from http://129.69.86.144/raptec/Reports/deliverables/Deli2_t42_all.PDF, 09.29, 27/6/2.
2. Choi, S.H. and Samavedam, S. Modelling and optimisation of rapid prototyping. *Computers in Industry*, 2002, Vol. 47, pp 39-53.
3. Berzins, M., Childs, T.H.C., Dalgarno, K.W., Ryder, G. and Stein, G. Densification and distortion in selective laser sintering of polycarbonate parts. In *Solid Freeform Fabrication Symposium 1995*, proceedings of the conference held in Austin, Texas, August 7-9, 1995, ISSN 1053-2153, pp. 196-203 (The University of Texas at Austin).
4. Childs, T.H.C., Berzins, M., Ryder, G., and Tontowi, A. Selective laser sintering of an amorphous polymer - simulations and experiments. *Proceedings of the IMechE Part B*, 1999, Vol. 213, pp 333-349.
5. Dalgarno, K.W., Childs, T.H.C., Rowntree, I. and Rothwell L., Finite element analysis of curl development in the selective laser sintering process, In *Solid Freeform Fabrication Symposium 1996*, proceedings of the conference held in Austin, Texas, August 12-14, 1996, ISSN 1053-2153, pp. 559-566 (The University of Texas at Austin).
6. Jamal, N.M. *Finite element analysis of curl development in the selective laser sintering process*. PhD Thesis, University of Leeds, 2001.
7. *ABAQUS/Standard Example Problems Manual Version 5.5*, Vol. 1, 1995, Hibbitt, Karlsson and Sorensen, Inc.
8. Ho, H., Gibson, I. and Cheung W. Effects of Energy Density on Bonus Z, Surface Roughness and Warpage of Selective Laser Sintered Polycarbonate, *Proceedings of the Eighth International Conference on Rapid Prototyping*, held in Tokyo, Japan, June 12-13, 2000, pp. 99-103.
9. Bushko, W. and Stokes, V. Solidification of Thermoviscoelastic Melts, Part 4: Effects of Boundary Conditions on Shrinkage and Residual Stresses. *Polymer Engineering and Science*, 1996, Vol. 36, pp. 658-675.
10. *ABAQUS/Standard User's Manual Version 5.8*, Vol. 2, 1998, Hibbitt, Karlsson and Sorensen, Inc.
11. *ABAQUS/Standard User's Manual Version 5.6*, Vol. 1, 1998, Hibbitt, Karlsson and Sorensen, Inc.
12. Ward, I.M. *Mechanical Properties of Solid Polymers*, 1985, Wiley.